

TERRESTRIAL ZONE DEBRIS DISK CANDIDATES IN h AND χ PERSEI

THAYNE CURRIE¹, SCOTT J. KENYON¹, GEORGE RIEKE², ZOLTAN BALOG^{2, 4}, & BENJAMIN C. BROMLEY³

Draft version February 1, 2008

ABSTRACT

We analyze 8 sources with strong mid-infrared excesses in the 13 Myr-old double cluster h and χ Persei. New optical spectra and broadband SEDs (0.36-8 μ m) are consistent with cluster membership. We show that material with $T \sim 300$ -400 K and $L_d/L_\star \sim 10^{-4}$ - 10^{-3} produces the excesses in these sources. Optically-thick blackbody disk models - including those with large inner holes - do not match the observed SEDs. The SEDs of optically-thin debris disks produced from terrestrial planet formation calculations match the observations well. Thus, some h and χ Persei stars may have debris from terrestrial zone planet formation.

Subject headings: planetary systems: formation planetary systems: protoplanetary disks

1. INTRODUCTION

Radiometric dating (Yin et al. 2002) suggests that the Earth had $\sim 90\%$ of its mass ~ 30 -40 Myr after the formation of the Sun. Terrestrial planet formation models suggest that most of this mass accumulation was complete by ~ 10 Myr and was dominated by mergers of moon-mass oligarchs (Kenyon & Bromley 2006, hereafter KB06; Chambers 2001). How terrestrial planets form around other stars is unresolved.

Optically-thin infrared (IR) emission from collisionally-produced debris is an important observational signature of planet formation (Kenyon & Bromley 2004, hereafter KB04; Rieke et al. 2005, hereafter R05; KB06). For a 1-2 M_\odot star, terrestrial planet formation should produce debris (and hence strong 5-10 μ m emission) for ≈ 10 -20 Myr. The 5-10 μ m signature of debris production should then begin to fade (KB04; R05; KB06). While many debris disk surveys (R05; Gorlova et al. 2006; Su et al. 2006) have discovered evidence for Kuiper-belt analogues from 24-70 μ m excess emission around early A stars, there have been fewer searches for terrestrial zone debris disks around ~ 1 -2 M_\odot stars. Previous searches (e.g. Meyer et al. 2006; Silverstone et al. 2006) have also concentrated on protoplanetary disks $\lesssim 5$ Myr old, or on the evolution of classical debris disks (ages $\gtrsim 30$ Myr) when planet formation is nearly complete and debris production is declining.

The double cluster h and χ Persei ($d=2.34$ kpc, ~ 13 Myr old) provides an ideal probe of terrestrial planet formation. The clusters contain $\gtrsim 5000$ stars with masses $\gtrsim 1.3 M_\odot$, an order of magnitude larger population than other nearby, evolved clusters. The recent IRAC 3.6-8 μ m survey of h and χ Persei by Currie et al. (2007; hereafter C07) discovered a large population of sources with IR excess emission in the IRAC bands (up to 4-8%

at 8 μ m). C07 showed that the frequency of disk emission is larger for less massive stars and at greater distances from the central star. The IR excesses are bluer, K_s -[IRAC] ~ 0.5 -1.5, than those for Class II T Tauri stars (e.g. Kenyon & Hartmann 1987; hereafter KH87), which suggests that the disks are less optically thick and perhaps in an evolved state.

The goal of this paper is to constrain the source of the excess IR emission in h and χ Per stars by modeling the SEDs and IRAC/MIPS colors of sources with high quality IR/optical photometry and spectra. In §2 we describe our sample and explain our SED fitting. In §3 we show that the IR excess is best explained by debris from terrestrial planet formation. Both photospheric emission and optically-thick disk models fail to explain the SED slopes and IRAC colors. Optically-thick disk + inner hole models are marginally consistent with photometry $\leq 5.8 \mu$ m but are not consistent with either the 8 μ m ([8]) data or MIPS data.

2. INFRARED PHOTOMETRY AND SPECTRAL TYPING

The C07 survey covered ~ 0.75 sq. deg. centered on h and χ Persei. We select stars with $J \leq 16$ and with 'strong excesses' at multiple IRAC bands, K_s -[5.8] ≥ 0.5 (or K_s -[4.5] ≥ 0.5 in absence of [5.8] data) and K_s -[8] ≥ 0.75 . All of these sources have $K_s \geq 13.5$. In this sample, 1,915 have 5σ detections at [5.8] (or [4.5]) and [8], lie along the h and χ Per isochrone, and were not flagged for contamination by background galaxies (see §2.3 of C07 for criteria). Eight of these sources (see Table 1) have 'strong excesses' and have high-quality optical photometry from Keller et al. (2001; UBVI) or Slesnick et al. (2002; V band only).

We derive a worst-case probability that the [5.8] and [8] emission from these 8 sources are contaminated by $z=0.1$ -0.4 PAH-emission galaxies that escaped flagging and could masquerade as a 'strong excess' source. We assume that all sources from our population are as faint as our faintest source ($K_s=15$) and that any superimposed galaxy with [5.8] ≤ 15 will trigger selection of one of the 1,915 sources. We also assume that all galaxies are PAH-emission galaxies, that none were removed by flagging, and that each star covers an 'area' of $\pi 2^2$ square arcseconds. Using the galaxy number counts for the Bootes field from Fazio et al. (2004; $\sim 1,165$ /sq. deg. for [5.8] ≤ 15), the expected number of contami-

¹ Harvard-Smithsonian Center for Astrophysics, 60 Garden St. Cambridge, MA 02140

² Steward Observatory, University of Arizona, 933 N. Cherry Av. Tucson, AZ 85721

³ Department of Physics, University of Utah, 201 JFB, Salt Lake City, UT 84112

⁴ on leave from Dept. of Optics and Quantum Electronics, University of Szeged, H-6720, Szeged, Hungary
 Electronic address: tcurrie@cfa.harvard.edu

nated sources is $N_p \sim 2.2$ ($\pi 2^2 \times 1165 / (3600^2) \times 1915$). If we adopt the number density of PAH-emission galaxies for this field (Stern et al. 2005) instead of the number density of *all* galaxies, the predicted number of contaminated sources is $N_p \sim 0.3$. Thus, even under the most pessimistic assumptions no more than $\sim 2/8$ sources are contaminated.

We obtained Hectospec (Fabricant et al. 2005) and FAST (Fabricant et al. 1998) spectra of these 8 sources on the 6.5m MMT and 1.5m Tillinghast telescope at F. L. Whipple Observatory during September-November 2006. For the FAST sources, we took ~ 10 minute exposures using a 300 g mm^{-1} grating blazed at 4750 \AA and a $3''$ slit. These spectra cover $3800\text{--}7500 \text{ \AA}$ at 6 \AA resolution. For each Hectospec source (the six faintest), we took three, 10-minute exposures using the 270 g mm^{-1} grating. This configuration yields spectra at $4000\text{--}9000 \text{ \AA}$ with 3 \AA resolution. The data were processed using standard FAST and Hectospec reduction pipelines (e.g. Fabricant et al. 2005). The resulting spectra typically have moderate signal-to-noise, $S/N \gtrsim 30$ per pixel (Figure 1a).

To measure spectral types, we derived spectral indices of H_α , H_β , H_γ , H_δ , the G band (4305 \AA), and Mg I (5175 \AA) as in O’Connell (1973). We derived piecewise linear relationships between spectral indices and spectral type from the Jacoby et al. (1984) standards, similar to the method of Hernandez et al. (2004). All sources have spectral types consistent with those expected for 13 Myr h & χ Persei sources reddened by $E(B-V) \sim 0.52$ (Bragg & Kenyon 2005) at a distance of 2.4 kpc. None are foreground M stars or background O/B stars. No sources have a H_α equivalent width $\geq 10 \text{ \AA}$ indicative of gas accretion. As an additional check on our spectral types, we fit the SED from U through K_s to photospheric models in λ vs. λF_λ space. Spectral types derived from spectroscopy and SED fitting agree to within 2-3 subclasses. To model their intrinsic SEDs through [8], the sources were dereddened in all bands. We use Bessell & Brett (1988) and Keller et al. (2001), respectively, to calibrate the V-I and U-B reddening from $E(B-V)$, and the IR extinction laws from Indebetouw (2005) to deredden the 2MASS and IRAC bands.

Finally, we acquired MIPS $24 \mu\text{m}$ photometry with an integration time of 80 seconds/pixel. The frames were processed using the MIPS Data Analysis Tool; PSF fitting in the IRAF/DAOPHOT package was used to obtain photometry adopting 7.3 Jy for the zero-point magnitude (Gordon et al. 2005). We derive the MIPS 5σ upper limits from the histogram of the number counts as a function of magnitude. The MIPS data are complete to ~ 10.5 and yield a 5σ detection for only one source, source 5, with $[24] \sim 9.9 \pm 0.05$. We estimate the [24] reddening from Mathis (1990): $A_{[24]} \approx 0.025$. Therefore, our one 5σ detection at [24] has $K_s\text{--}[24] \sim 4.4$.

3. MODELING OF DISK EMISSION

Figure 2 shows the source SEDs (filled diamonds). To compare them with stellar photospheres, we used optical/IR colors for each spectral type from Kenyon & Hartmann (1995; KH95) and converted from colors to λF_λ in the Johnson-Cousins system. The zero-point flux from the models was scaled to match the dereddened V through J fluxes for each source (Allen 2001; Cohen et

al. 2003). All sources have photospheric fluxes through [3.6]; one source (4) clearly has IR excess at [4.5]. All sources with [5.8] and [8] measurements show clear evidence for circumstellar emission. The SEDs are similar to some ‘anemic’ disks around A-F stars in IC 348 (Lada et al. 2006).

To characterize the emission, we calculate the dust blackbody temperatures that match the observed [8] flux but do not overproduce the flux at other wavelengths. The range of dust blackbody temperatures (typically 300-400 K) for each source imply terrestrial zone emission. Derived disk luminosities are $L_d/L_\star \sim 10^{-4}\text{--}10^{-3}$, comparable to debris disks (R05).

To investigate the disk emission in more detail, we constructed three disk models spanning a range of evolutionary states for disks surrounding ~ 10 Myr old stars. The optically thick, non accreting, flat disk model (KH87) assumes that the disk passively reradiates photons from the star and extends from the magnetospheric truncation radius to $\gtrsim 2000 R_\star$. In a second disk model, an ‘inner hole’ model, all disk material $\leq 50 R_\star$ ($\sim 1 \text{ AU}$ for $R=2 R_\odot$, this was the best fit) from the star is removed from the optically thick, flat disk model. This model is similar to the morphology expected for ‘transition’ T Tauri disks (e.g KH95).

Finally, we model the IR emission from an optically-thin debris disk. In a debris disk, modest IR excesses result from small grains produced by destructive collisions between $\sim 1\text{--}10 \text{ km}$ planetesimals during the oligarchic growth stage of planet formation (see KB04; Kenyon & Bromley 2005). As in the KB04 calculations, the starting radial surface density (Σ) profile follows a minimum mass solar nebula, $\Sigma \propto r^{-3/2}$ (Hayashi 1981). Planetesimal collisions are modeled in the terrestrial zone, $\sim 1.5\text{--}7.5 \text{ AU}$ away from a $2M_\odot$ primary star. Disk emission is tracked for $\sim 100 \text{ Myr}$ from the start of collisions. The resulting SED is computed and 2MASS and IRAC colors are determined.

Figure 2 compares predictions from the three disk models to the data (Figure 2). Optically-thin, debris disk models (dash-three dot line) consistently match the [5.8] and [8] IRAC fluxes. While the debris disk models can overpredict the flux at [3.6] and [4.5] by $\sim 25\%$, the predictions at [5.8] and [8] typically fall within 20% of observed values. In some cases (sources 2-4, 8) the agreement is excellent. Standard optically-thick disk models (long dashes, source 1 only) and the best-fit optically-thick disk + inner hole models (dashes) fail to match the SEDs. The optically-thick disk models overestimate the flux by \geq a factor of 10 beyond [3.6]. The inner hole model matches the observed SEDs through [3.6] but typically overpredicts the [5.8] ([8]) fluxes by factors of 1.5 (3). Furthermore, the optically-thick flat disk and inner hole models consistently predict a $24 \mu\text{m}$ flux $\sim 10\text{--}20\times$ greater (or ~ 3 magnitudes redder) than the observed flux (one source) or the 5σ upper limits (5 sources). The debris disk model, which predicts $K_s\text{--}[24] \sim 3$, is consistent with the $24 \mu\text{m}$ upper limits of the sources not detected with MIPS. The debris disk prediction is ~ 2.5 times fainter (~ 1 magnitude bluer) than the observed $K_s\text{--}[24]$ color from source 5. However, planet formation calculations at 30-150 AU predict significant $24 \mu\text{m}$ emission ($K_s\text{--}[24] \approx 3.5\text{--}4$) by $\sim 10\text{--}30 \text{ Myr}$ around $2 M_\odot$ stars

(Currie et al. in prep., Kenyon & Bromley, in prep.), so regions beyond the terrestrial zone may contribute some [24] emission. More massive disks or those with flatter density profiles (e.g. r^{-1}) than assumed here may also yield slightly larger [24] excesses.

Figure 3 shows the results in K_s -[4.5]/ K_s -[8] and K_s -[5.8]/ K_s -[8] color-color diagrams. In both figures, the IRAC colors of our sources (diamonds/triangles) lie halfway between the photospheric and inner hole models (left square and dotted line). At the peak of debris disk emission (solid line), the debris disk model also produces IR colors about halfway between the photospheric and inner hole models. The colors show good agreement with debris disk predictions in K_s -[5.8] and K_s -[8], typically within 0.2 mags, and fair agreement with the [4.5] data. Inner hole models for earlier (later) spectral types predict K_s -[8] ~ 1.75 (3), or ~ 1 -2 magnitudes too red. Many of the sources are, at best, marginally consistent with any star+background galaxy colors (dot-dashed enclosed region): 3/7 (4/7) are consistent with contamination in the K_s -[4.5]/ K_s -[8] (K_s -[5.8]/ K_s -[8]) diagrams. Only 2/8 are consistent with contamination in both plots. Even considering systematic errors/uncertainties (model uncertainties, photometric errors), the sources occupy a very small region of possible star+galaxy colors and are still only marginally consistent with contamination.

The optically thick disk+inner hole model fails to model the IRAC/MIPS data in all cases; the debris disk model is consistent with the IRAC data and more consistent with the MIPS detection/upper limits. Thus, debris from planet formation is the most plausible explanation for near-to-mid IR emission from these sources.

4. DISCUSSION

Near-to-mid IR-excess emission for our sample originates from dust with $T \sim 300$ -400 K and $L_d/L_* \sim 10^{-4}$ - 10^{-3} . Circumstellar debris produced from terrestrial planet formation is the most likely explanation for this emission. Future observations with the Spitzer Space Telescope and the James Webb Space Telescope can provide stronger constraints on the SEDs of these terrestrial zone debris disk candidates and greatly expand the sample of ~ 13 Myr-old candidates in η and χ Persei. Current IRAC/MIPS data require that the disks have little dust out to distances probed by [4.5] and are optically thin out to [24]. For a 13 Myr, K0 (F1) star with a luminosity of ~ 1.49 (7.4) L_\odot , the disks are dust free out to ~ 0.23 (0.51) AU and optically thin to ~ 6.6 (14.6) AU. Deeper MIPS [24] observations of these sources may more conclusively constrain the disk SED to compare with debris disk and transition disk models. Mid-IR spectroscopy may also aid source identification from the ~ 10 -20 μm flux levels and the strength of the 10 μm silicate feature (see Sicilia-Aguilar et al. 2007).

We thank Matt Ashby, Rob Gutermuth, and Anil Seth for useful discussions regarding galaxy contamination and the anonymous referee for a thorough review. We acknowledge support from the NASA Astrophysics Theory Program grant NAG5-13278, TPF Grant NNG06GH25G and the Spitzer GO program (Proposal 20132). T. C. received funding from an SAO Predoctoral Fellowship; Z. B. received support from Hungarian OTKA Grants TS049872, T042509, and T049082. This work was supported by contract 1255094, issued by JPL/Caltech to the University of Arizona.

REFERENCES

- Allen, C. W., 2001, *Allen's Astrophysical Quantities*, Fourth Ed., Arthur N. Cox (ed.), Springer-Verlag
- Bessell, M., Brett, J., 1988, *PASP*, 100, 1134
- Bragg, A. & Kenyon, S., 2005, *ApJ*, 130, 134
- Chambers, J., 2001, *Icarus*, 152, 205
- Cohen, M., et al., 2003, *AJ*, 126, 1090
- Currie, T., et al., 2007, *ApJ*, 659, 599
- Fabricant, D., et al., 1998, *PASP*, 110, 79
- Fabricant, D., et al., 2005, *PASP*, 117, 1411
- Fazio, G., et al., 2004, *ApJS*, 154, 39
- Gordon, K. D., et al., 2005, *PASP*, 117, 503
- Gorlova, N., et al., 2006, *ApJ*, 649, 1028
- Hayashi, C., 1981, *Prog. Theor. Phys. Suppl.*, 70, 35
- Hernandez, J., et al., 2004, *AJ*, 127, 1682
- Jacoby, G., et al., 1984, *ApJS*, 56, 257
- Keller, S.C., et al., 2001, *AJ*, 122, 248
- Kenyon, S., Bromley, B., 2004, *ApJL*, 602, 133
- Kenyon, S., Bromley, B., 2005, *AJ*, 130, 269
- Kenyon, S., Bromley, B., 2006, *AJ*, 131, 1837
- Kenyon, S., Hartmann, L., 1987, *ApJ*, 323, 714
- Kenyon, S., Hartmann, L., 1995, *ApJS*, 101, 117
- Indebetouw, R., et al., 2005, *ApJ*, 619, 931
- Mathis, J., 1990, *ARA&A*, 28, 37
- Meyer, M., et al., 2006, *astro-ph/0606399*
- O'Connell, R., 1973, *AJ*, 78, 1074
- Lada, C.J., et al., 2006, *AJ*, 131, 1574
- Rieke, G., et al., 2005, *ApJ*, 620, 1010
- Sicilia-Aguilar, A., et al., 2007, *astro-ph/0701321*
- Silverstone, M., et al., 2006, *ApJ*, 639, 1138
- Slesnick, C., et al., 2002, *ApJ*, 576, 880
- Stern, D., et al., 2005, *ApJ*, 631, 163
- Su, K., et al., 2006, *ApJ*, 653, 675
- Yin, Q., et al., 2002, *Nature*, 418, 949

TABLE 1
SOURCES ANALYZED IN THIS PAPER (DEREDDENED, $A_V \sim 1.62$)

#	α	δ	ST	V	U-B	B-V	V-I	J	H	K_s	[3.6]	[4.5]	[5.8]	[8]	[24]
1	2:17:34.7	56:47:25	F1	14.15	-	-	-	13.58	13.51	13.52	13.38 \pm 0.01	13.29 \pm 0.05	12.97 \pm 0.05	12.15 \pm 0.04	-
2	2:17:38.0	56:53:51	A9	14.03	0.09	0.17	0.06	13.61	13.55	13.45	-	-	12.55 \pm 0.06	12.35 \pm 0.14	-
3	2:19:11.3	57:09:53	F1	14.72	0.46	0.37	0.34	13.88	13.64	13.64	13.31 \pm 0.03	13.23 \pm 0.02	13.23 \pm 0.11	12.89 \pm 0.08	>10.5
4	2:22:06.4	57:07:06	F7	15.44	-	-	0.51	14.62	14.22	14.28	-	13.77 \pm 0.19	-	13.38 \pm 0.12	>10.5
5	2:19:07.7	57:14:05	F9	15.77	0.35	0.63	0.53	14.65	14.26	14.29	14.27 \pm 0.06	14.19 \pm 0.09	13.83 \pm 0.10	13.03 \pm 0.09	9.9
6	2:17:59.3	56:53:45	G9	16.40	-	-	0.45	15.15	14.60	14.87	14.71 \pm 0.07	14.73 \pm 0.11	14.27 \pm 0.13	14.06 \pm 0.19	>10.5
7	2:17:39.5	57:20:26	K0	16.43	-	-	0.76	14.85	14.43	14.69	14.43 \pm 0.06	14.50 \pm 0.05	14.29 \pm 0.18	13.68 \pm 0.14	>10.5
8	2:17:46.0	57:10:18	K1	16.72	-	-	0.78	15.12	14.54	14.43	14.59 \pm 0.09	14.35 \pm 0.10	14.03 \pm 0.11	13.51 \pm 0.12	>10.5

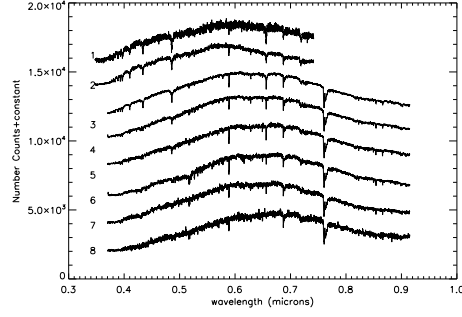


FIG. 1.— FAST and Hectospec spectra for our sample, with spectral types ranging from F1/A9 (top) to K0/K1 (bottom). The bottom source (8) has a 2000 count offset; spectra near the edges approach zero counts.

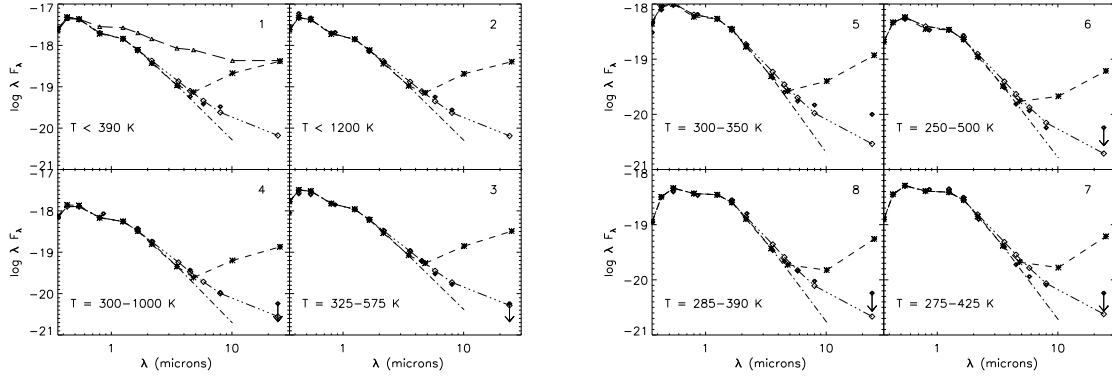


FIG. 2.— Spectral energy distributions of the sources. Filled diamonds denote detections; down arrows identify MIPS 5σ upper limits. The SED fits from V through $[3.6]$ match photospheric predictions (dot-dashed line). Sources have clear, strong IR excess at $[5.8]$ and $[8]$. The dust blackbody temperatures indicate terrestrial zone emission. Both standard optically-thick flat disk models (shown in the first plot only, large dashed line/open triangles) and optically-thick models with inner holes (dashed line/asterisks) overpredict the flux at $[8]$. Debris disk models (three dot-dashed line/open diamonds) appear to be consistent with the data.

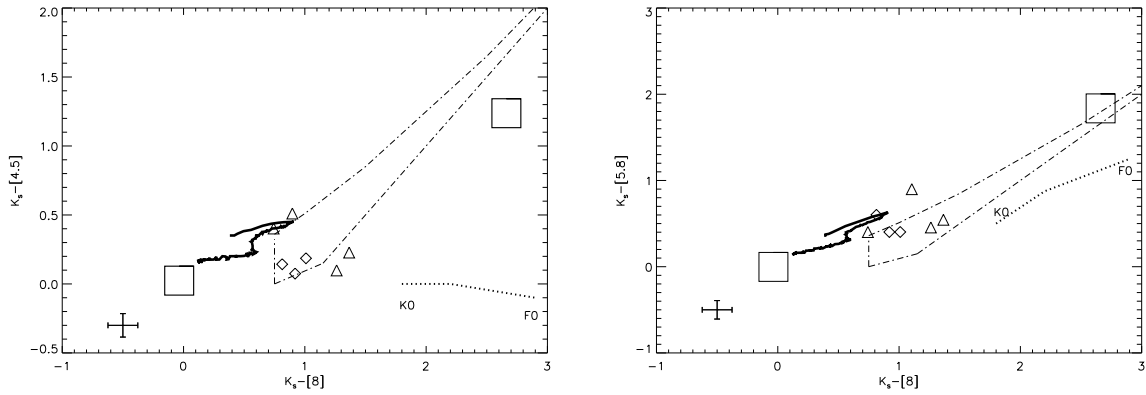


FIG. 3.— K_s -[IRAC] colors for sources —triangles for sources earlier than G2, diamonds for sources later— and predictions for photospheric, and standard optically-thick disk models (left and top-right squares), and a range of optically-thick disk + inner hole models (K0 to F0). The median errors in IRAC are shown in the lower left-hand corner. The photospheric and optically-thick disk colors are for a spectral type of G2 and vary little with spectral type. Overplotted as a thick solid line are the expected colors for emission produced by optically-thin debris, a byproduct of terrestrial planet formation. The debris disk colors change due to the evolving dust production rate from planet formation. The dot-dashed region encloses possible colors for photospheric sources+background galaxy contamination; PAH galaxies have $[5.8]-[8]=1-3$ and any star+galaxy composite 'source' with $[4.5,5.8]-[8] \gtrsim 1$ would have been flagged as a contaminated source and removed from our sample. The debris disk model fits to within ~ 0.3 mags in all cases; only 2/8 sources are consistent with star+PAH galaxy-contaminated colors.